

A coumarin based fluorescent probe for NIR imaging guided photodynamic therapy against *S. aureus*-induced infection in mice models

Jun Li,^{#, a, b} Le Tu,^{#, c} Qingying Ouyang,^{#, c} Sheng-gang Yang,^{#, d} Xiao Liu,^a Qianqian Zhai,^a Yao Sun,^c Juyoung Yoon,^{*, b} Huailong Teng^{*, a}

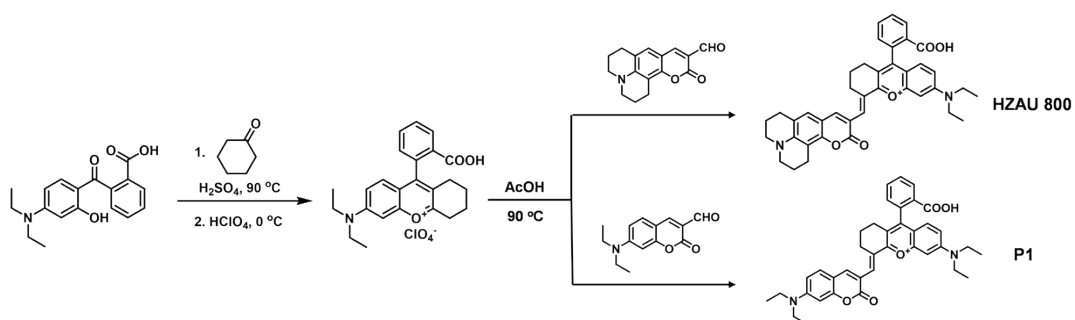
- a. Department of Chemistry, College of Science, Huazhong Agricultural University, Wuhan 430070, P. R. China.
- b. Department of Chemistry and Nano Science, Ewha Womans University, Seoul 120-750, Korea.
- c. Key Laboratory of Pesticides and Chemical Biology, Ministry of Education, College of Chemistry, Central China Normal University, Wuhan 430079, P. R. China.
- d. College of Pharmacy, Guizhou Medical University, Guiyang, 550025, P. R. China.

J. Li, L. Tu, Q. Ouyang and S. Yang contributed equally to this work.

Table of Contents

Content	Page#
1. Synthesis and characterization of probe HZAU800 and P1	S2-S5
2. pH dependence and photostability of HZAU800	S5
3. Verification of ROS produced by HZAU800	S6
4. Cytotoxicity assay	S6
5. NIR imaging of <i>S. aureus</i> and <i>E. colic</i> using HZAU800	S7
6. Evaluation of PDT effect of HZAU800 on <i>S. aureus</i> infected tissues	S7
7. The H&E staining assessment of HZAU800 in different tissues	S8
8. The dihedral angle and molecular dynamics simulation of HZAU800	S8
9. Reference	S8

1. Synthesis and characterization of probe HZAU800 and P1



General synthetic procedure. Rhodamine analog **1**¹ (1.0 eq) and coumarin derivatives (1.0 eq)^{2,3} were dissolved in AcOH (8 mL). The mixture was heated at 90 °C for 5 h. After completing the reaction, the solvent was removed under reduced pressure, the residue was subjected to column chromatography (CH₂Cl₂: MeOH=15:1) to obtain the final product as green solid.

HZAU800: yield: 16.5%. ¹H NMR (400 MHz, CD₃CN) δ 8.26 (d, *J* = 8.0 Hz, 1H), 8.13 (s, 1H), 7.89 (s, 1H), 7.83 (t, *J* = 7.6 Hz, 1H), 7.74 (t, *J* = 7.6 Hz, 1H), 7.26 (d, *J* = 7.6 Hz, 1H), 7.07-6.98 (m, 4H), 3.65-3.59 (m, 4H), 3.35 (t, *J* = 5.2 Hz, 4H), 2.90 (t, *J* = 6.0 Hz, 2H), 2.78 (t, *J* = 6.4 Hz, 2H), 2.74 (t, *J* = 6.0 Hz, 2H), 2.33 (m, *t, J* = 5.6 Hz, 4H), 1.82-1.74 (m, 4H), 1.26 (s, 6H). ¹³C NMR (150 MHz, DMSO-*d*₆): 166.73, 161.14, 151.19, 147.59, 144.12, 133.40, 130.29, 129.52, 128.57, 127.64, 126.99, 121.95, 119.37, 113.18, 108.35, 105.35, 95.64, 65.00, 59.85, 54.99, 49.75, 49.20, 45.35, 27.20, 26.87, 25.37, 21.05, 20.74, 19.79, 19.66, 15.25, 14.17, 12.59. HRMS: calcd. for [M-ClO₄]⁺: 627.28535; found: 627.28540.

P1: yield: 13%. ¹H NMR (600 MHz, CDCl₃): 7.94 (d, *J* = 11.4 Hz, 1H), 7.64-7.62 (m, 1H), 7.58-7.52 (m, 2H), 7.38 (s, 1H), 7.28 (s, 1H), 7.19 (d, *J* = 11.4 Hz, 1H), 6.61-6.58 (dd, *J* = 3.0, 13.2 Hz, 1H), 6.53 (d, *J* = 3.0 Hz, 1H), 6.49-6.45 (m, 2H), 6.35-6.33 (dd, *J* = 3.6, 13.8 Hz, 1H), 3.43 (q, *J* = 10.8 Hz, 4H), 3.35 (q, *J* = 10.8 Hz, 4H), 2.71-2.69 (m, 1H), 2.15-2.09 (m, 1H), 1.72-1.58 (m, 4H), 1.22 (t, *J* = 10.2 Hz, 6H), 1.17 (t, *J* = 10.2 Hz, 6H). ¹³C NMR (150 MHz, DMSO-*d*₆): 169.08, 161.33, 155.51, 150.66, 141.56, 135.38, 130.67, 130.49, 130.00, 129.84, 129.47, 128.38, 126.55, 123.28, 115.71, 109.32, 108.12, 96.59, 96.48, 44.21, 43.80, 40.14, 27.09, 31.83, 12.44. HRMS: calcd for [M-ClO₄+H]⁺: 604.2926; found: 604.2884.

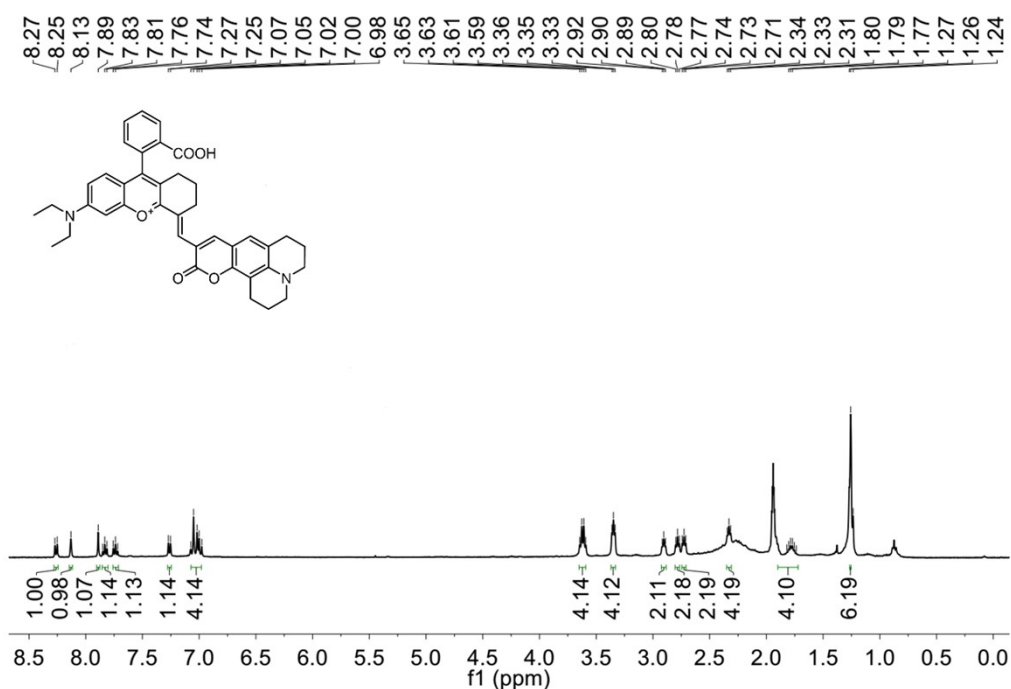


Figure S1. ¹H NMR of HZAU800

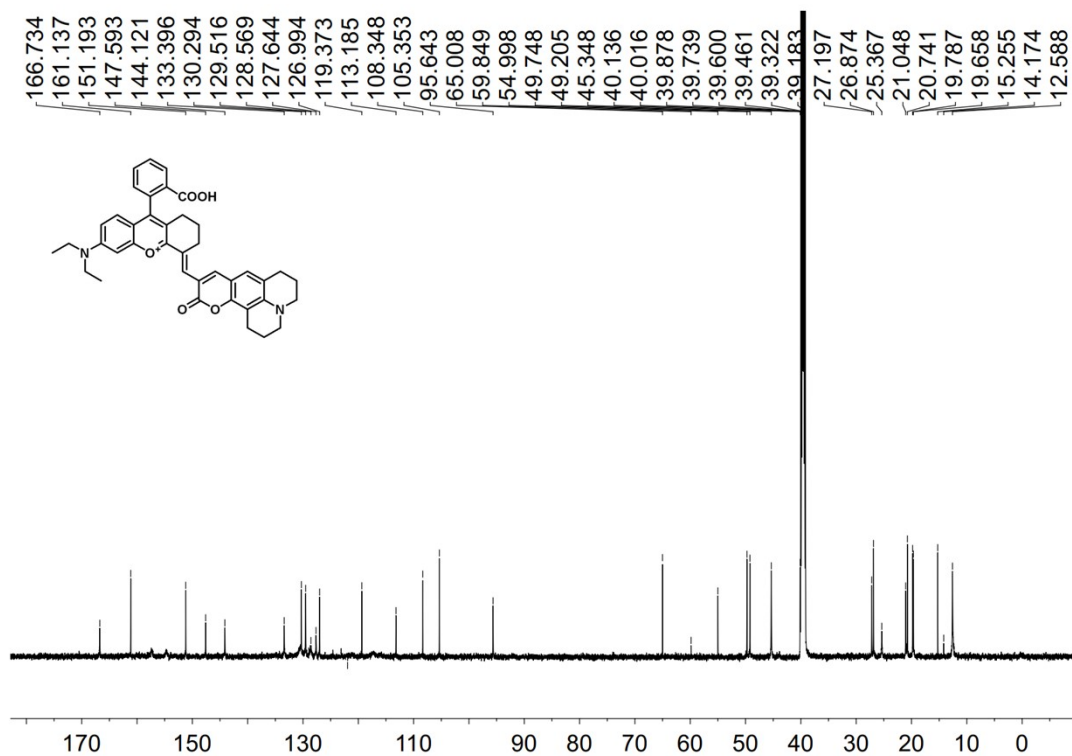


Figure S2. ¹³C NMR of HZAU800

T: FIMS+p ESI Full lockms [80.0000-1200.0000]

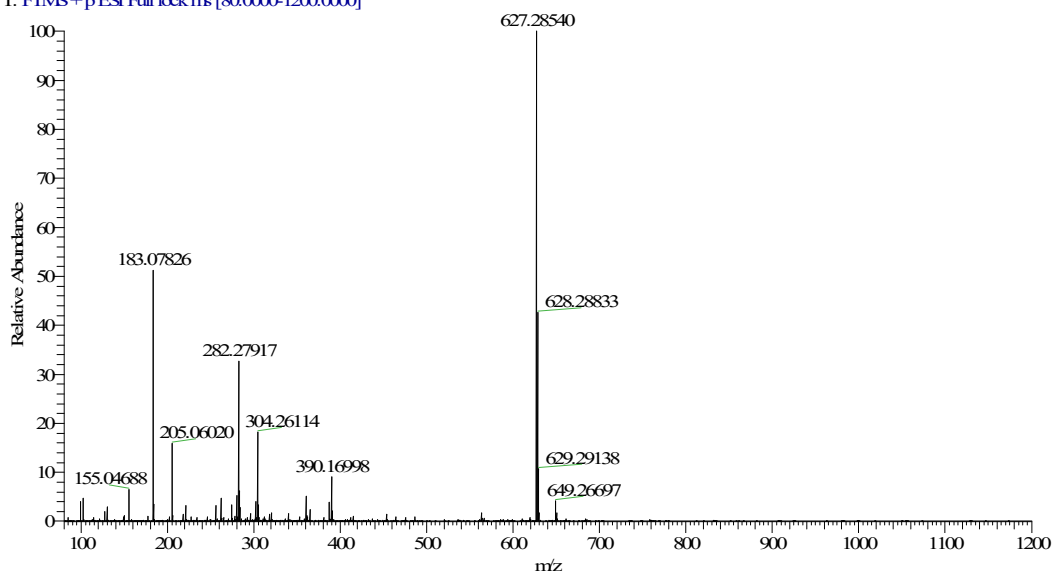


Figure S3. HRMS of HZAU800

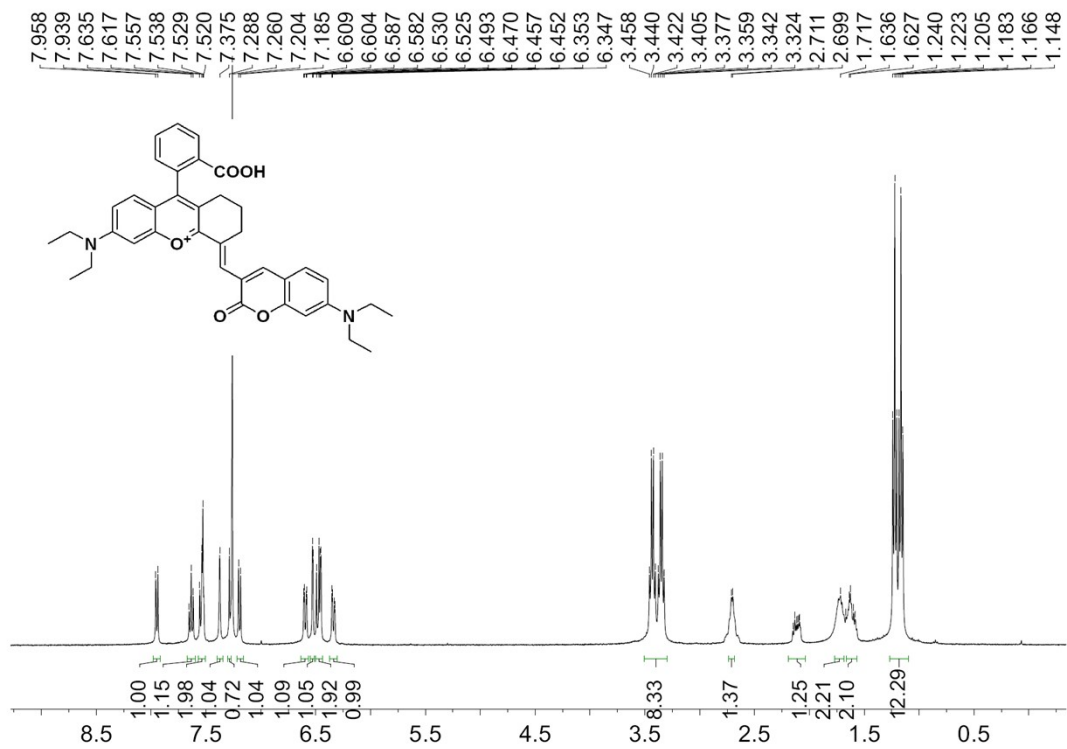


Figure S4. ¹H NMR of P1

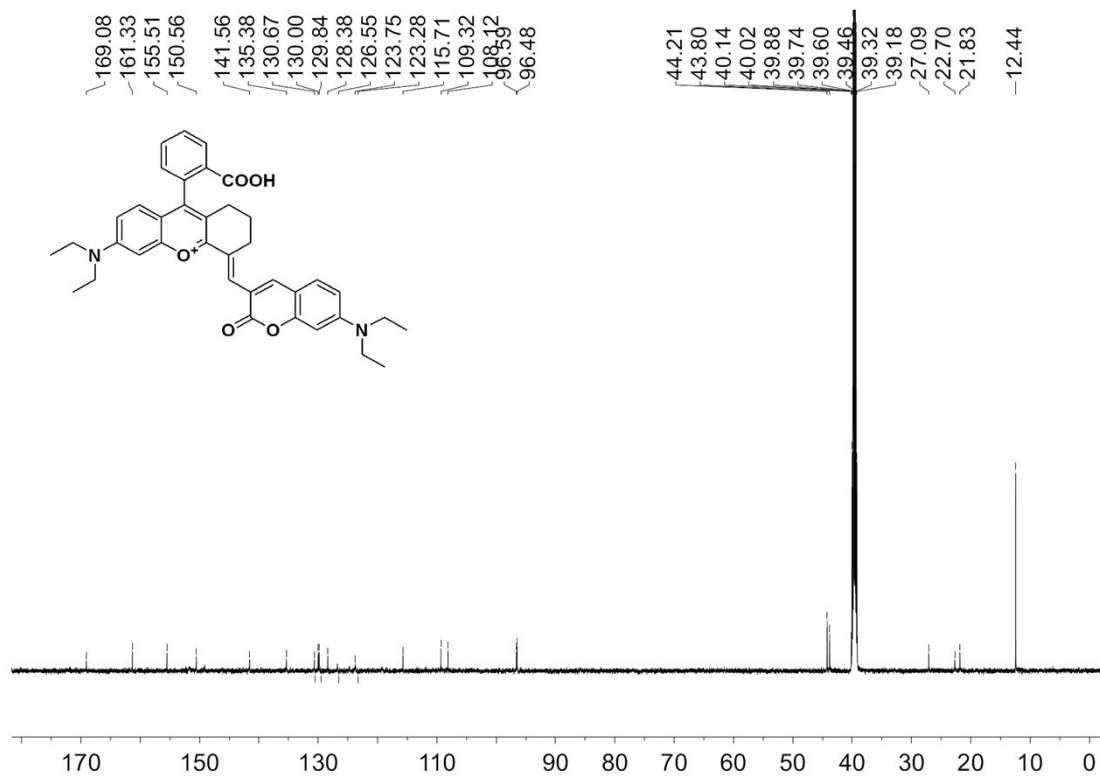


Figure S5. ¹³C NMR of P1

OYQY-2 #13 RT: 0.09 AV: 1 NL: 2.36E8
T: FTMS+p ESI Full lock.ms [80.0000-1200.0000]

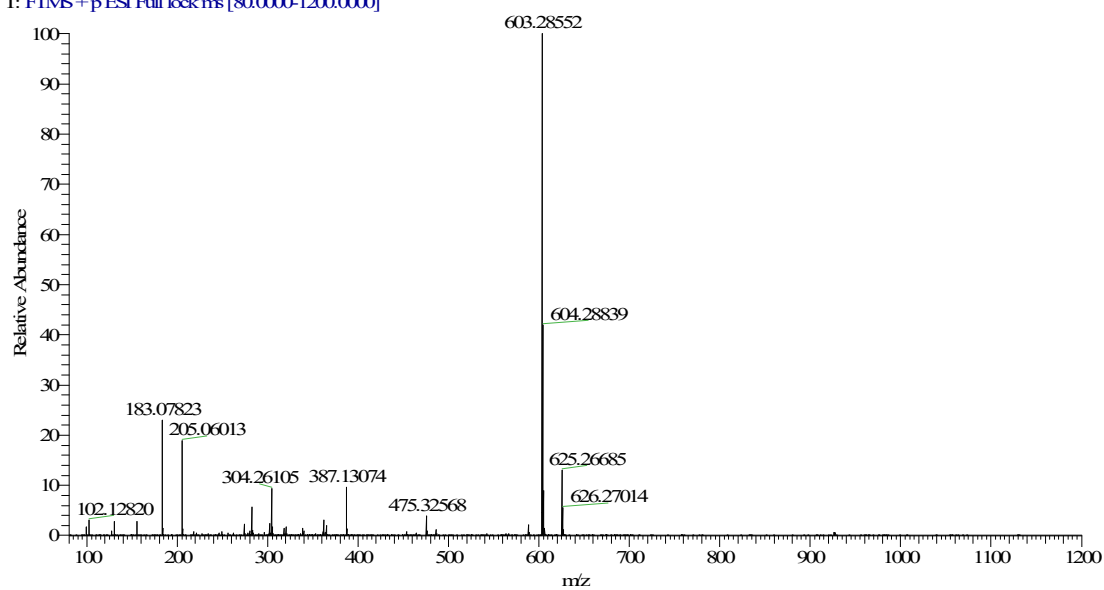


Figure S6. HRMS of P1

2. Optical properties of HZAU800

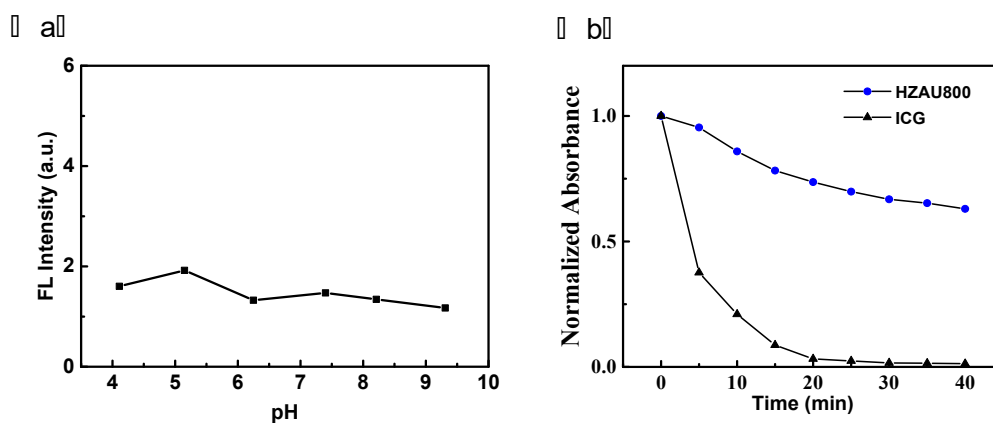


Figure S7. pH dependence (a) and photostability of HZAU800 (b)

3. Verification of ROS produced by HZAU800

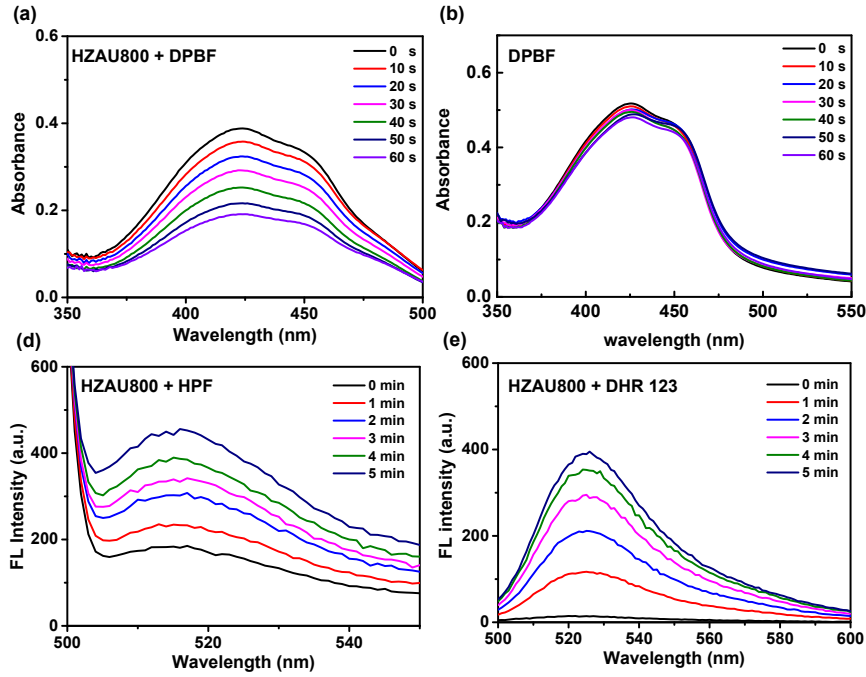


Figure S8. Verification of ROS produced by **HZAU800** using different ROS indicators: (a) UV spectrum of 10 μM **HZAU800** + 30 μM DPBF under laser's irradiation at different time; (b) UV spectrum of 30 μM DPBF under laser's irradiation at different time; (c) fluorescence response of 10 μM **HZAU800** + 10 μM HPF under laser's irradiation at different time; (d) fluorescence response of 10 μM **HZAU800** + 10 μM DHR 123 under laser's irradiation at different time.

4. Cytotoxicity assay

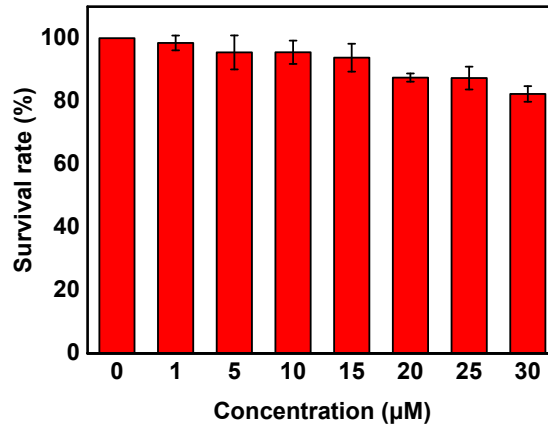


Figure S9. Cytotoxicity data of **HZAU800** (0, 1, 5, 10, 15, 20, 25, 30 μM) in HeLa cells.

5. NIR imaging of *S. aureus* and *E. colic* using HZAU800

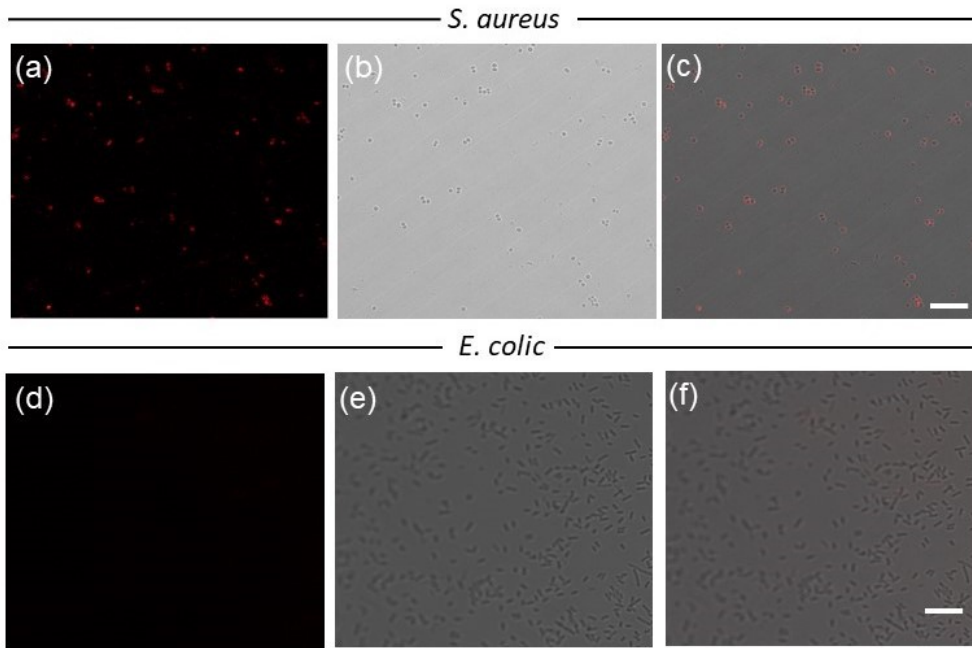


Figure S10. NIR imaging of HZAU800 (40 $\mu\text{g}/\text{mL}$) in *S. aureus* and *E. colic* with dark field (a) and (d), bright field (b) and (e), merged field (c) and (f), scale bar: 10 μm .

6. Evaluation of phototherapeutic effects of HZAU800 on *S. aureus* infected tissues

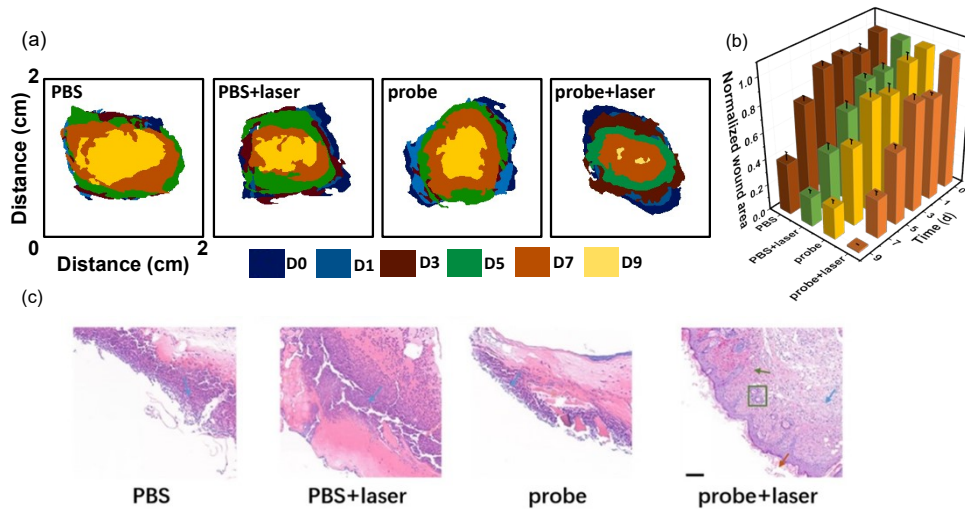


Figure S11. (a) and (b) the distance and area of *S. aureus*-infected wounds after different treatments; (c) The hematoxylin and eosin (H&E) staining assessment of *S. aureus*-infected tissues after different treatments, blue arrow: neutrophils, green arrow: fibroblast; green rectangle: granulation tissue. Scale bar: 100 μm .

7. The H&E staining assessment of HZAU 800 in different tissues

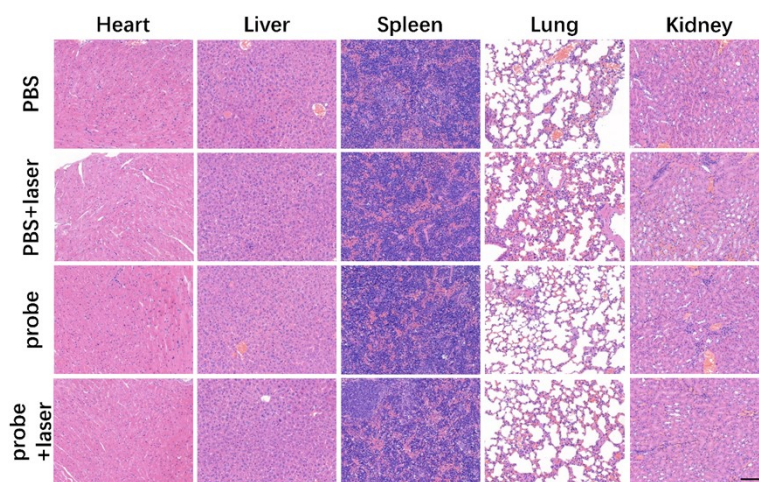


Figure S12. The H&E staining assessment of HZAU800 in different tissues. Scale bar: 100 μm .

8. The dihedral angle and molecular dynamics simulation of HZAU800

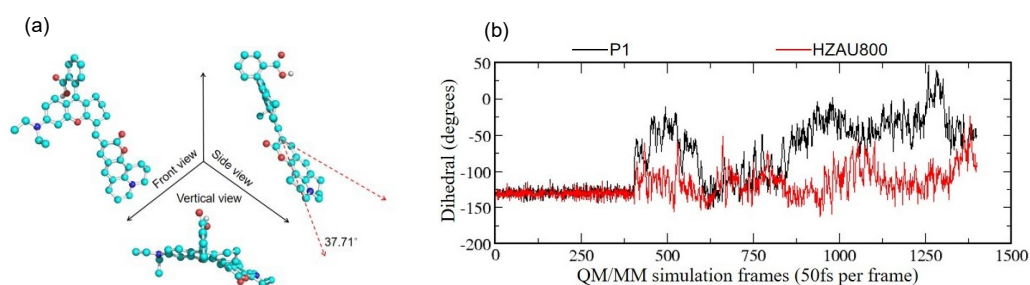


Figure S13. (a) the dihedral angle of HZAU800; (b) the molecular dynamics simulation of HZAU800 and P1.

9. Reference

- (1) L. Yuan, W. Lin, Y. Yang and H. Chen, A unique class of near-infrared functional fluorescent dyes with carboxylic-acid-modulated fluorescence ON/OFF switching: rational design, synthesis, optical properties, theoretical calculations, and applications for fluorescence imaging in living animals. *J. Am. Chem. Soc.*, 2012, **134**, 1200-1211.
- (2) J. Li, Y. Cui, C. Bi, S. Feng, F. Yu, E. Yuan, S. Xu, Z. Hu, Q. Sun, D. Wei and J. Yoon, Oligo (ethylene glycol)-functionalized ratiometric fluorescent probe for the detection of hydrazine in vitro and in vivo. *Anal. Chem.* 2019, **91**, 7360-7365.
- (3) Y. Liang, Y. Zhao, C. Lai, X. Zou and W. Lin, Coumarin-based TICT fluorescent probe for real-time fluorescence lifetime imaging of mitochondrial viscosity and systemic inflammation in vivo. *J. Mater. Chem. B*, 2021, **9**, 8067-8073.